




ANN CONTROL FOR IMPROVED PERFORMANCE OF WIND ENERGY SYSTEM CONNECTED TO GRID

Brijesh KUMAR¹ , Kanwarjit Singh SANDHU² , Rahul SHARMA¹ 

¹School of Renewable Energy and Efficiency, National Institute of Technology,
136119 Kurukshetra, Haryana, India

²Electrical Engineering Department, National Institute of Technology,
136119 Kurukshetra, Haryana, India

kumarbrijesh92@gmail.com, kjssandhu@rediffmail.com, rahulsharma.knit2006@gmail.com

DOI: 10.15598/aece.v20i4.4474

Article history: Received Feb 11, 2022; Revised Jun 15, 2022; Accepted Jul 22, 2022; Published Dec 31, 2022.
This is an open access article under the BY-CC license.

Abstract. This paper proposes the novel control strategy to improve the power quality injection of wind energy system using Doubly Fed Induction Generator (DFIG) into the grid by implementing artificial neural network. The torque ripple produced in DFIG due to loading by grid tied inverter, which leads to poor power quality injection into the system. Also, these ripples transferred by DC link and causes heating losses and generator phase current distortion. Therefore, this paper modelled ANN based control scheme to reduce the torque ripple content and restrict the transfer of ripple by DC link to improve the outcome of wind energy system while operating in variable conditions. The DFIG system under studied are modelled and simulated in MATLAB SIMULINK to verify the improvement using proposed control strategy. The recent control technique is also simulated for reflecting the effectiveness in the proposed control method. The outcomes obtained are studied and analysed with the existing control scheme to highlight the improvement obtained by proposed control.

Keywords

ANN, DFIG, grid integration, power quality, renewable, wind energy system.

1. Introduction

In the last decade, there has been an exponential growth in the utilization of renewable energy resources in power systems. It eliminates the limitations of

fossil fuels like production of harmful gases, energy dependency, challenge to meet the growing demand of energy consumption etc. Also, renewable energy is freely present in nature and can be utilized in any corner of the globe. Hence, the use of renewable energy may become the best suited alternative in place of conventional sources. Recent literature indicates wind power generation has played and will continue to play a crucial role in renewable energy field for the coming years. DFIG based Wind Energy Conversion Systems (WECS) are very popular in wind energy utilization and widely used for wind power generation due of their efficient, reliable, and variable speed nature [1]. DFIG offers some important advantages over permanent magnet synchronous generator such as wide range of operation ($\pm 30\%$ of the rated speed), better power factor and can be controlled, robust, reduced noise, suited for high rating applications, reduced switching losses, reduced converter size and cheaper as compared to PMSG [2].

There are lot of control strategies discussed in the literature to implement WECS having DFIG generator to improve efficiency, power quality, frequency support to grid, power smoothing etc. The control schemes commonly used are mainly Vector Control (VC) or Field-Oriented Control (FOC), Direct Torque Control (DTC) and Direct Power Control (DPC) and their evolved version over a period [3] and [4]. There are issues in VC like proper decoupling problem, very sensitive towards control parameters due to several cascaded loops in control design, which introduce stability issue under wide operating range and slower dynamic response, are reported in [5]. Similarly, DTC have demerits of high torque ripple, poor transient

behaviour, complicated online calculations, and instability over wide operating range are also reported in some recent literature [6]. Some literature proposed DPC of DFIG based WECS to mitigate the demerits and further enhance the quality of power of the grid interfaced wind energy system [7]. DPC control has the same control structure as DTC, but it regulates the active and reactive power by using the rotor and stator flux effects [8]. There are some demerits of DPC control like requirement of high-power loss in converter switching and the complexity while designing of the filters for variable switching frequency are highlighted [9].

Some recent literature highlighted that the signals generated by PI controllers to control the converters are not effectively contributed to the decoupling of d-q axis variables [5]. Also, the drawback associated with PI controller is its limitation over operating region, which makes system unstable under wide parametric variations [10]. Therefore, recent research advocates the use of intelligent control to deal with unknown dynamics, mutual coupling, disturbances, and improved performance & robustness of system against wide operating and environmental variations of renewable sources [11].

Artificial Neural Networks (ANN) have the potential to effectively handle the nonlinearity and parametric uncertainties because of inherent property to predict the system complexity and enhance the performance [12]. In [13] and [14], a fuzzy control integrating with neural networks is proposed for tuning and is implemented in the control structure to improve the generation and the response of the DFIG system. In [15], a control of ANN based PI controller is given to enhance the stability of DFIG under asymmetrical faults, which reflects the effectiveness of the ANN based scheme. In [16], a comparative study has been conducted between an ANN based PI controller and a classical one to summarize the merits and demerits of both the controllers while implementing in the DFIG system in variable loading. In [17], an intelligent controller is designed based on the probabilistic fuzzy neural network for the regulation of active and reactive power to a reference to maintain the support provided to the grid. In [18], a fault detection and identification are discussed to indicate the voltage using a neural network for improving the capability in low voltage operations of the DFIG. The results discussed in [17] and [18] indicate the enhanced performance of the proposed strategy; however, the proposed algorithm is validated only for small scale systems. Similarly, the Multilayer Perceptron (MLP) design for the control of DFIG using DPC structure is reported in [19]. The MLP controller uses ANN to eliminate the parameter designing of PI and further reduces the complexity in the control structure to achieve better regulation of active and reactive power without the need of PI and table for switching.

The recent literature suggested that ANN has not been utilized yet to mitigate the ripple content in the torque and enhance the power smoothing. Therefore, the challenges and the merits of ANN motivated us to design a novel ANN based control strategy for DFIG connected to grid. This paper proposes an ANN based solution for the torque ripple and power smoothing problem associated to DFIG based WECS. The DC link is controlled, and frequency support is provided to the grid using proposed ANN based DPC scheme to achieve the above-mentioned objectives. The results are compared with PI controller based DPC scheme to reflect the effectiveness. The proposed and conventional schemes are implemented on the WECS interfaced with the grid as shown in Fig. 1. The GSC and RSC blocks in the figure represent grid side and rotor side converters, respectively. The dq to abc or abc to dq blocks are used to transform the three-phase quantity into synchronous reference frame to control d and q independently. PLL block is used to synchronize the transformations according to the respective voltage reference and angle. SVM block is utilized to generate gating pulses for converters using space vector modulation. The proposed ANN controller is implemented to control active and reactive power of DFIG, which is explained in Sec. 3.

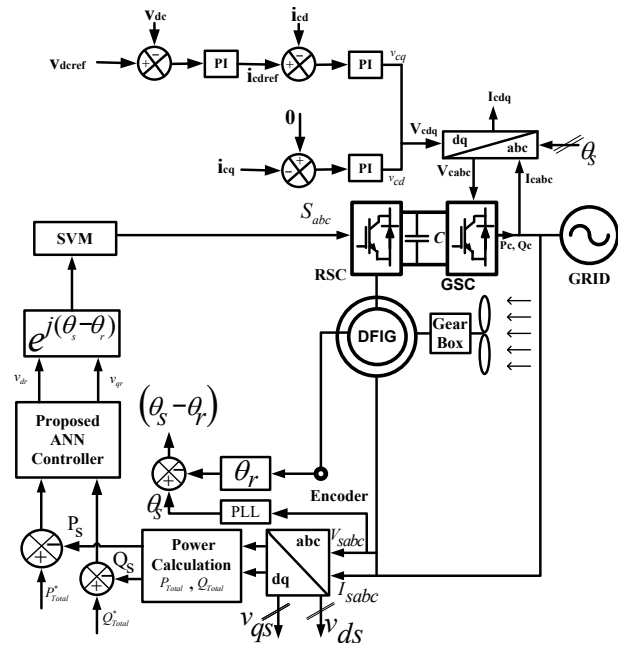


Fig. 1: Structure of WECS and conventional control.

The paper is categorised as follows: a brief review of ANN used in this paper and their design is presented in Sec. 2. A mathematical modelling and designing of the proposed control for DFIG based WECS is discussed in Sec. 3. Results and their effectiveness have been presented using comparative analysis in Sec. 4. At last, the findings of the study are

concluded and highlighted the key outcomes of the proposed work in Sec. 5.

2. DFIG Modelling and Artificial Neural Network

The mathematical modelling of the DFIG in DQ reference frame can be derived using the equivalent circuit as shown in Fig. 2.

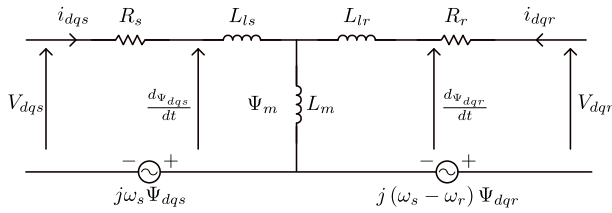


Fig. 2: DFIG equivalent circuit in the d-q reference frame.

The voltage, flux, and power equations of the rotor side and grid side converters for DFIG based wind energy system can be written [20] in the DQ reference frame as:

$$v_{ds} = R_s i_{ds} + \frac{d\psi_{ds}}{dt} - j\omega_s \psi_{qs}, \tag{1}$$

$$v_{qs} = R_s i_{qs} + \frac{d\psi_{qs}}{dt} + j\omega_s \psi_{ds}, \tag{2}$$

$$v_{dr} = R_r i_{dr} + \frac{d\psi_{dr}}{dt} - j(\omega_s - \omega_r) \psi_{qr}, \tag{3}$$

$$v_{qr} = R_r i_{qr} + \frac{d\psi_{qr}}{dt} + j(\omega_s - \omega_r) \psi_{dr}. \tag{4}$$

Equation (1), Eq. (2), Eq. (3) and Eq. (4) are representing stator side and rotor side voltages of DFIG in DQ reference frame. The notations are defined as ψ_{ds} , ψ_{qs} , ψ_{dr} and ψ_{qr} are the stator and rotor flux in rotating reference dq frame, respectively. Further, L_s , L_m and L_r are the inductances of stator, magnetizing and rotor, respectively. ω_s is taken as the frequency in electrical domain, while ω_r is the mechanical angular frequency, v_{ds} , v_{qs} , i_{ds} and i_{qs} are the stator voltage and current in rotating reference dq frame respectively. Similarly, v_{dr} , v_{qr} , i_{dr} and i_{qr} are the rotor voltages and currents, respectively. The resistances of the stator and rotor side are taken as R_s and R_r , respectively.

Similarly, stator and rotor flux can be written [21] as:

$$\psi_{ds} = L_s i_{ds} + L_m i_{dr}, \tag{5}$$

$$\psi_{qs} = L_s i_{qs} + L_m i_{qr}, \tag{6}$$

$$\psi_{dr} = L_r i_{dr} + L_m i_{ds}, \tag{7}$$

$$\psi_{qr} = L_s i_{qr} + L_m i_{qs}, \tag{8}$$

whereas $L_s = L_m + L_{ls}$ and $L_r = L_m + L_{lr}$.

The stator and rotor side power flow in grid connected DFIG system can also be written in DQ frame as:

$$P_s = \frac{3}{2} \text{Re}(\bar{v}dq_s \cdot \bar{i}^*dq_s) = \frac{3}{2} (v_{ds}i_{ds} + v_{qs}i_{qs}), \tag{9}$$

$$Q_s = \frac{3}{2} \text{Im}(\bar{v}dq_s \cdot \bar{i}^*dq_s) = \frac{3}{2} (v_{qs}i_{ds} - v_{ds}i_{qs}), \tag{10}$$

$$P_r = \frac{3}{2} \text{Re}(\bar{v}dqr \cdot \bar{i}^*dqr) = \frac{3}{2} (v_{dr}i_{dr} + v_{qr}i_{qr}), \tag{11}$$

$$Q_r = \frac{3}{2} \text{Im}(\bar{v}dqr \cdot \bar{i}^*dqr) = \frac{3}{2} (v_{qr}i_{dr} - v_{dr}i_{qr}), \tag{12}$$

where, P_s and Q_s are taken as the active and reactive power of stator side. P_r and Q_r are the active and reactive power of rotor side. Similarly, generator electromagnetic torque developed can be written as:

$$T_{em} = p \cdot (\psi_{ds} \cdot i_{qs} - \psi_{qs} \cdot i_{ds}), \tag{13}$$

where, T_{em} is the electromagnetic torque, p is the pole.

In this paper, feedforward ANN [11] is used with Back Propagation (BP) algorithm. The basic working schematic diagram of the BP network is given in Fig. 3.

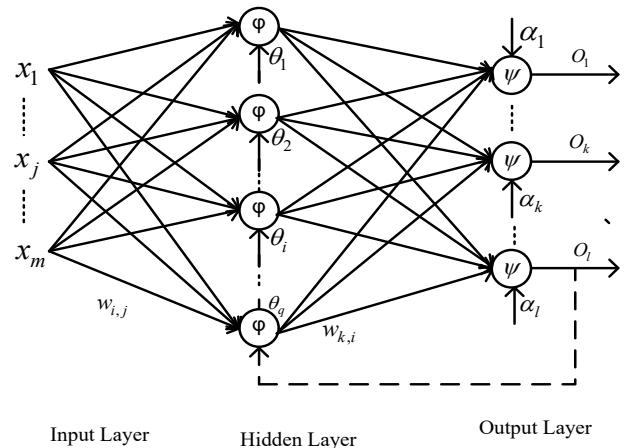


Fig. 3: Structure of feedforward BP neural network.

The structure having three layers as input, hidden, and output. Hidden layer can be multiple in numbers per the requirement and problem formulation. Input layer contains the input values of the network. Input is processed by artificial neurons of hidden and output layers.

There are weights and bias associated with each neuron as parameters and used by neurons in non-linear calculations to process the information. Example of the i^{th} neuron may be taken in the hidden layer; the weight is represented as w_{ij} while threshold is denoted as θ_i . Now, j is the subscript of input ($j = 1, 2, \dots, m$) while i is the neuron subscript ($i = 1, 2, \dots, q$). Therefore, the equation can be mathematically written as Eq. (14) and Eq. (15):

$$net_i = \sum_{j=1}^m w_{ij}x_j + \theta_i, \tag{14}$$

where, net_i are the linear part of the expression and the non-linear nature of the neuron is shown by Eq. (15).

$$y_i = \varphi(net_i) = \varphi\left(\sum_{j=1}^m w_{ij}x_j + \theta_i\right), \quad (15)$$

where, the output is defined as y_i , and φ is an excitation functions to incorporate the non-linear behaviour of neurons. The commonly used functions are S-shaped tangent function (tansig), S-shaped logarithmic function (logsig), and a pure linear function (purelin).

Similar calculations are done by the output layer of neurons and finally k^{th} output o_k in this example may be written as:

$$o_k = \psi(net_k) = \psi\left[\sum_{i=1}^q w_{ki}\varphi\left(\sum_{j=1}^m w_{ij}x_j + \theta_i\right) + a_k\right], \quad (16)$$

where, the weight and bias are denoted as W_{ki} and a_k of neuron k in the output layer, respectively while the excitation function is denoted as φ . The selection of weights of the neuron does not have any defined procedure. There are different techniques given in literatures like random weight selection, zero weight selection, Xavier initialization etc. In this paper, Xavier initialization has been used to update the weights by initialling them randomly.

3. Proposed ANN Based DPC Control Design

The rotor side and grid side controls are designed in this section using ANN to regulate active & reactive power as well as maintain DC link voltage constant. Therefore, the power equations are written as:

$$P_{Total} = P_s + P_r, \quad (17)$$

$$Q_{Total} = Q_s + Q_r, \quad (18)$$

where, P_{Total} is the total active power delivered to grid by DFIG based WECS, P_s is the active power injected through the stator side into the grid, while P_r is the rotor side active power. Similarly, Q_{Total} is the total reactive power of the DFIG.

The active and reactive power control is established by considering the stator flux alignment on the d-axis and subsequently, quadrature component of stator flux is zero. Therefore, $\varphi_{ds} = \varphi_s$ and $\varphi_{qs} = 0$.

Therefore, the electromagnetic torque can be simplified and written as:

$$T_{em} = -p \cdot \frac{L_m}{L_s} \psi_{ds} i_{qr}. \quad (19)$$

Similarly, the stator side active power can be rewritten by neglecting the stator resistance.

Hence, v_{ds} and $v_{qs} = v_s$.

$$P_S = -v_S \frac{L_m}{L_s} i_{qr}. \quad (20)$$

Similarly, stator side reactive power can be rewritten as:

$$Q_S = \frac{v_s \psi_s}{L_s} i_{dr} - v_s \frac{L_m}{L_s} i_{dr}. \quad (21)$$

Also, the rotor voltages can be rewritten according to the rotor currents as:

$$\begin{cases} v_{dr} = R_r i_{dr} + \left(L_r - \frac{L_m^2}{L_s}\right) \frac{di_{dr}}{dt} + \\ -s \cdot \omega_s \left(L_r - \frac{L_m^2}{L_s}\right) i_{qr}, \\ v_{qr} = R_r i_{qr} + \left(L_r - \frac{L_m^2}{L_s}\right) \frac{di_{qr}}{dt} + \\ +s \cdot \omega_s \left(L_r - \frac{L_m^2}{L_s}\right) i_{dr} + s \cdot \omega_s \frac{L_m v_s}{\omega_s L_s}, \end{cases} \quad (22)$$

with $s = \frac{(\omega_s - \omega_r)}{\omega_s}$.

Now, neglecting the voltage drops for slip values, which are relatively very low, we can modify the Eq. (22) and written as:

$$\begin{cases} v_{dr} \approx 0, \\ v_{qr} \approx s \frac{L_m v_s}{L_s}. \end{cases} \quad (23)$$

Using the Eq. (10) and Eq. (11), the rotor active and reactive power can be rewritten by substituting Eq. (23), this leads to:

$$\begin{cases} P_r = s \cdot \frac{L_m v_s}{L_s} \cdot i_{qr}, \\ Q_r = s \cdot \frac{L_m v_s}{L_s} \cdot i_{dr}. \end{cases} \quad (24)$$

Hence, the total active and reactive powers involved in the grid are expressed by Eq. (17) and Eq. (18), can be simplified by substituting Eq. (20), Eq. (21) and Eq. (24) as:

$$\begin{cases} P_{Total} = (s - 1) \cdot v_s \cdot \frac{L_m}{L_s} \cdot i_{qr}, \\ Q_{Total} = \frac{v_s^2}{\omega_s L_s} + (s - 1) \cdot v_s \cdot \frac{L_m}{L_s} \cdot i_{dr}. \end{cases} \quad (25)$$

The total power that needs to be regulated by the rotor side converter control to achieve the better performance as compared to conventional one is expressed

by Eq. (25). Therefore, ANN based optimal training control is designed and implemented by discretizing the Eq. (25) and can be written as:

$$\left\{ \begin{array}{l} P_{Total}(k+1) = (s-1) \cdot v_s(k+1) \cdot \frac{L_m}{L_s} \cdot i_{qr}(k+1), \\ Q_{Total}(k+1) = \frac{v_s(k+1)^2}{\omega_s L_s} + (s-1) \cdot v_s(k+1) \cdot \frac{L_m}{L_s} \cdot i_{dr}(k+1). \end{array} \right. \quad (26)$$

Now, the $(k+1)$ is the predicted value of the next sample and need to be find mathematically. But stator windings are directly connected to the grid that guarantees the stator voltage to be maintained constant and equal to the grid voltage.

Hence:

$$v_s(k+1) = v_s(k). \quad (27)$$

Now, $i_{qr}(k+1)$ and $i_{dr}(k+1)$ can be calculated by discretizing the Eq. (22) and expressed as:

$$\begin{aligned} i_{dr}(k+1) &= i_{dr}(k) + T_s M [v_{dr}(k) - i_{dr}(k)R_r] + \\ &\quad + T_s s \omega_s i_{qr}(k), \\ i_{qr}(k+1) &= i_{qr}(k) + T_s M [v_{qr}(k) - i_{qr}(k)R_r] + \\ &\quad - T_s s \omega_s i_{dr}(k) - T_s M s \frac{L_m v_s(k)}{L_s}, \end{aligned} \quad (28)$$

where, $M = \left(L_r - \frac{L_m^2}{L_s} \right)$ and sampling time is T_s .

Now, the constraint is considered as the output voltage of inverter (RSC). The inverter output amplitude is depending on the value of the input DC voltage, hence inequality formed as written in Eq. (29).

$$-V_{dc} < v(k) < V_{dc}. \quad (29)$$

To sum-up the above-mentioned discrete equations, optimization problem can be formulated as Eq. (30), and the initialization of all the variables are considered zero:

$$\left\{ \begin{array}{l} \text{Minimize obj} = \\ \left\{ \begin{array}{l} \sum_{k=0}^m (P_{Total}^*[k+1] - P_{Total}[k+1])^2 \\ \sum_{k=0}^m (Q_{Total}^*[k+1] - Q_{Total}[k+1])^2 \end{array} \right\} \end{array} \right. \quad (30)$$

Subjected to Eq. (26), Eq. (27), Eq. (28) and Eq. (29) and initial conditions.

The above optimization problem is solved by a specific optimization solver and used to identify the optimal positions of v_{dr} , v_{qr} , i_{dr} and i_{qr} for the

desired active and reactive power regulation. The optimal values in p.u. are given in Tab. 1.

Similarly, Grid Side Converter (GSC) is utilized to regulate the DC link voltage at the desired set level. The ANN control is designed to maintain DC link voltage using the discretizing of power balancing equation between input DC power availability on the GSC and the GSC output power injected into the grid or vice versa from the rotor side.

Now, the power balancing dynamic equation of the DC link capacitor:

$$\left(C_{dc} \frac{dv_{dc}}{dt} \right) v_{dc} = (v_{gd}i_{gd} + v_{gq}i_{gq}), \quad (31)$$

where, V_{dc} is the DC link voltage, C_{dc} is the DC link capacitor, V_{gd} & V_{gq} are the grid side d & q axis voltages, while i_{gd} & i_{gq} are the grid side d & q axis currents of the GSC, respectively.

$$v_{dc}(k+1) = v_{dc}(k) + \frac{T_s [(v_{gd}(k)i_{gd}(k) + v_{gq}(k)i_{gq}(k))]}{C_{dc}v_{dc}(k)}. \quad (32)$$

Similarly, grid current dynamic equations using inductance-filter in d - q axis are discretized and expressed as:

$$\begin{aligned} i_{gd}(k+1) &= i_{gd}(k) + T_s \left[\frac{r_g i_{gd}(k)}{L_f} + \right. \\ &\quad \left. + \omega_s i_{gq}(k) \right] + T_s \left(\frac{v_{gd}(k)}{L_f} - \frac{u_{gd}(k)}{L_f} \right), \end{aligned} \quad (33)$$

$$\begin{aligned} i_{gq}(k+1) &= i_{gq}(k) + T_s \left[\frac{r_g i_{gq}(k)}{L_f} + \right. \\ &\quad \left. + \omega_s i_{gd}(k) \right] + T_s \left(\frac{v_{gq}(k)}{L_f} - \frac{u_{gq}(k)}{L_f} \right), \end{aligned} \quad (34)$$

where, L_f is the inductance of the GSC filter, r_g is the filter resistance, while u_{gd} and u_{gq} are the GSC output voltages before filter. The optimization problem formulation for the DC link voltage control using above equations Eq. (32), Eq. (33) and Eq. (34) can be represented as:

$$\text{Minimize obj} = \sum_{k=0}^m (V_{dc}^*[k+1] - V_{dc}[k+1])^2, \quad (35)$$

subjected to equation Eq. (32), Eq. (33) and Eq. (34) and initial conditions.

The PSO optimization algorithm is utilized to find the optimal values are given in Tab. 1 using the objective function given in equation Eq. (30) by considering the initial conditions as zero and taking constraints into account like minimum and maximum values of the variables and active as well as reactive powers. These optimal values are used to train the ANN block for the control of DFIG based WECS.

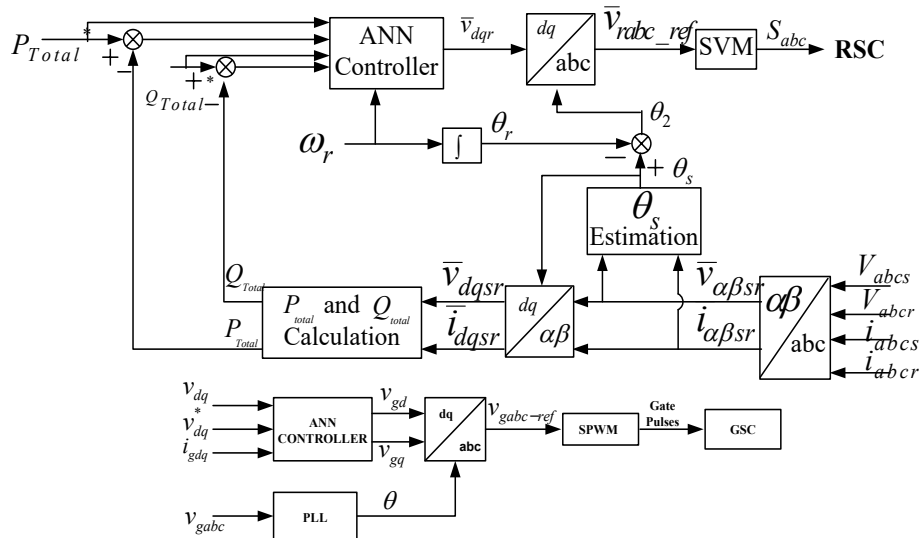


Fig. 4: Proposed ANN control scheme for WECS.

Tab. 1: Optimal data for training of rotor side neural network.

P_{Total}^*	Q_{Total}^*	v_{dr}	v_{qr}	i_{dr}	i_{qr}
0.45	0	-0.0535	-0.0117	0.4364	-0.272
0.60	0	-0.1366	-0.0285	0.5688	-0.276
0.73	0	-0.1809	-0.0416	0.6619	-0.281
0.88	0	-0.2054	-0.0526	0.7850	-0.288
0.91	0	-0.2072	-0.0643	0.8251	-0.262
0.90	0.1	-0.2155	-0.0613	0.8222	-0.375
0.90	0.15	-0.2227	-0.0620	0.8180	-0.431
0.88	0.20	-0.2226	-0.0636	0.7710	-0.476
0.88	0.25	-0.2317	-0.0668	0.7791	-0.520
0.73	0.25	-0.1975	-0.0475	0.6396	-0.536
0.73	0.30	-0.2006	-0.0489	0.6357	-0.589
0.60	0.35	-0.1545	-0.0317	0.5486	-0.644
0.45	0.35	-0.0746	-0.0184	0.4755	-0.643
0.45	0.45	-0.0744	-0.0198	0.4685	-0.744
0.37	0.45	0.0059	-0.0119	0.3941	-0.740
0.37	0.50	-0.0002	-0.0128	0.3977	-0.791

Tab. 2: Optimal data for training of grid side neural network.

V_{DC}^*	i_{gd}	i_{gq}	u_{gd}	u_{gq}
1	-0.0061	0	1.008	0.0359
1	-0.0412	0	1.029	0.0580
1	-0.0905	0	1.017	0.0703
1	-0.1157	0	1.027	0.0727
1	-0.1201	0	1.037	0.0820
1	-0.1080	0	1.041	0.0806
1	-0.1136	0	1.049	0.0791
1	-0.1000	0	1.061	0.0800
1	-0.0935	0	1.029	0.0536
1	-0.1088	0	1.011	0.0442
1	-0.0499	0	1.048	0.0535
1	-0.0102	0	1.057	0.0469
1	-0.0109	0	1.053	0.0453
1	0.0487	0	1.052	0.0420
1	0.0098	0	1.026	0.0440

Tab. 3: Parameters of ANN.

Variables taken as ANN input	$v_{dr}, v_{qr}, i_{dr}, i_{qr}, i_{gd}, i_{gq}, u_{gd}, u_{gq}$
Output Variables	$V_{rabc_ref}, U_{gabc_ref}$
Hidden layers	2
Number of neurons	16
Excitation Function	Tansig

Similarly, the cost/objective function given in equation Eq. (35) is solved using the same method as mentioned above for the optimal values value using optimization algorithm and the optimal values of i_{gd} & i_{gq} and u_{gd} & u_{gq} have been found to train the ANN block for the grid side control. The values in p.u. are given in Tab. 2.

The optimization results of Tab. 1 & Tab. 2 reflect the optimal control design under the given circumstances. Hence, the ANN is trained by the optimal data to learn such optimal control actions. The data sets given in table 1 and 2 are used for training and validation in a proportion of 80/20 percentage, respectively. The main objective of the proposed ANN control design is to replicate the type of optimal control behaviour under real time implementations. So, BP neural network is used in this paper to control RSC as well as GSC. The parameters used in the BP network are given in Tab. 3.

The chosen ANN is trained using the optimal data and after that it is ready to use in the system for the control of RSC and GSC to achieve the desired control objectives of the DFIG based WECS as shown in Fig. 4.

4. Results and Discussion

The effectiveness of the proposed method has been analysed in this section with the help of results taken under different operating and environmental condi-

tions. The 1.5 kW DFIG based WECS model has been considered under study and conventional DPC as well as proposed ANN control scheme is implemented. The parameters of the system under consideration have been given in Tab. 4.

Tab. 4: WECS and control parameters.

DFIG Power Rating	1.5 MW
Frequency	50 Hz
Voltage	690 V
Pole Pairs	2
Stator Resistance, R_s	$2.59 \cdot 10^{-3}$
Rotor Resistance, R_r	$2.89 \cdot 10^{-3}$
Stator Inductance, L_s	5.586 mH
Rotor Inductance, L_r	5.586 mH
Mutual Inductance, L_m	2.5 mH
DC link Voltage	1200 V
DC link Capacitance	900 μ F
Filter Inductance, L_f	300 mH

The incorporation of environmental change of wind speed is shown in Fig. 5 with wind speed changes at 4 s as the input of wind turbine to analyse the results. Wind speed varies from $8 \text{ m}\cdot\text{s}^{-1}$ to $14 \text{ m}\cdot\text{s}^{-1}$ at 4 s is observed in the simulation.

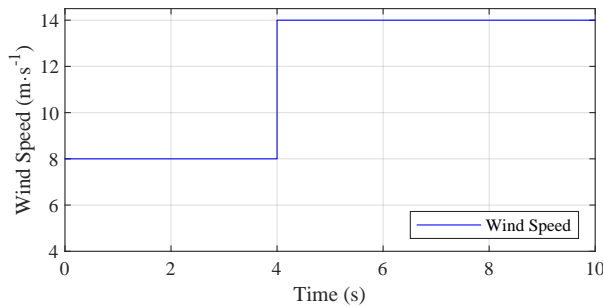


Fig. 5: Waveform of Wind Speed variation in WECS.

The generation of active power by WECS and injection into the grid is shown in Fig. 6. The variation in active power is clearly visible from 0.25 to 1 p.u at 4 s due to the variation in wind speed. The control schemes are utilized to analyse the WECS behaviour under change in wind speed in terms of active power. The waveforms yield different dynamic & transient behaviour under proposed and conventional techniques, respectively. The proposed ANN control scheme shows overall better results because it settles in lesser time and introduces low overshoot during transient operation. Also, a better output is observed as it damps the oscillations faster and has low ripple content as compared with conventional.

Similarly, the performance in front of reactive power has also been tracked as shown in Fig. 7 with the proposed ANN and conventional DPC control schemes where the change is introduced in reference of reactive power at 2 s. In terms of proposed scheme, the waveform is showing better power quality in the figure as transients & dynamics behaviour are good and

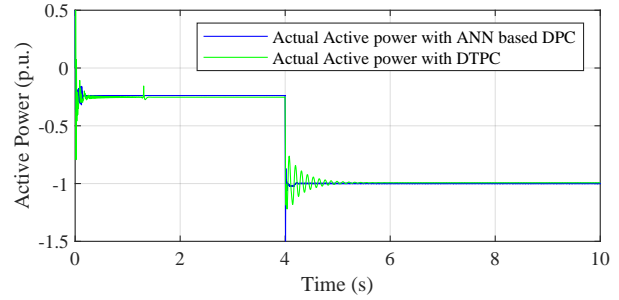


Fig. 6: Active power waveform of DFIG based WECS.

better settling time during steady state to reach the reference reactive power. Also, the ripple in the waveform is reduced as compared to the conventional one. On the other hand, conventional control scheme is showing poor settling time and having steady state error after the settling time. The response is sluggish, and the transient peak is above the maximum limit which reflects the poor control operation during transient and steady state operations of WECS.

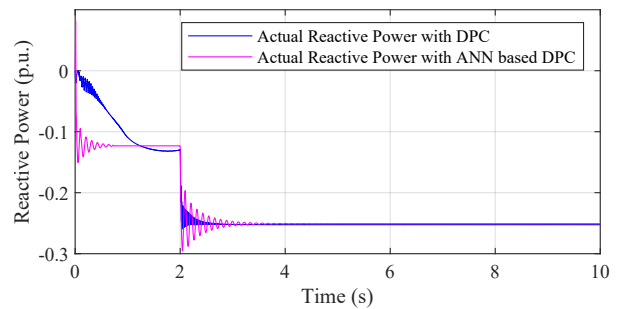


Fig. 7: Reactive power waveform of DFIG based WECS.

In Fig. 8, rotor current behaviour is shown in the waveforms with both the control schemes. The rotor current is clearly showing satisfactory results with both the control schemes. The waveform is transient condition at 4 s due to change in active power and varying frequency because of variation in rotor speed at 4 s. ANN provides performs better during transients in rotor current than conventional method, but the margin of improvement is negligible.

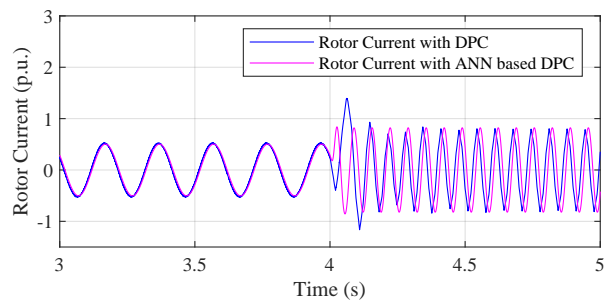


Fig. 8: Rotor current waveform of the DFIG based WECS.

Figure 9 shows the behaviour of DC link voltage waveform. The control schemes performances are compared, and the outcome is visible here. The proposed ANN control has an overall better output and shows highly impressive transient & dynamic performance to maintain DC link voltage at the desired level. Conventional DPC has a poor transient response as ripples is heavily introduced in the waveform, while time taken to reach the steady state is large and there is also slight steady state error present after 4 s. The ripples occur in waveform during conventional control which transfers the disturbance towards the turbine/generator side and creates stress issues as well as small fluctuations from the steady state speed. The proposed scheme is mitigating the ripple to avoid the abovementioned issues as can be clearly seen in Fig. 9.

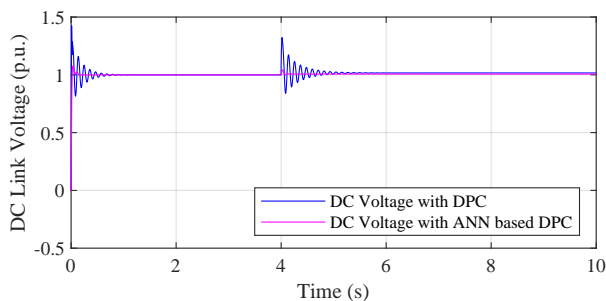


Fig. 9: Waveform of DC link voltage regulation in WECS.

The grid interaction and subsequent performance has been analysed by both the control strategies and the waveforms are shown in Fig. 10. The current waveform of the grid shows the quality of power being injected by WECS. The variation in the grid current is 4 s due to the increase in power output by the variation in wind speed. In this front also, ANN based control presents a better outcome compared to the conventional DPC with low ripple and better performance. Conventional DPC is also produces satisfactory results, but the proposed ANN based control gives a slightly better result.

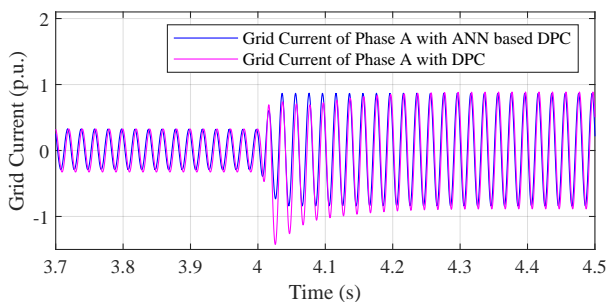


Fig. 10: Grid current waveform of the DFIG based WECS.

5. Conclusion

This paper elaborates an ANN based control solution for WECS connected to the grid to improve the system performance under different operating criterion. The outcomes have been shown to reflect the improvement in the operation of WECS while interfaced with the grid during the utilization of proposed control scheme. In terms of power quality, ANN based control produces lower disturbances, and hence, produces better quality of power. Further, it reduces the ripple distortion and shows effective response under transients. Also, the error mitigates the steady state time and reduces settling time against the conventional one. Therefore, this analysis concludes that the choice of optimal training data set is very important to get the better the outcome of the ANN based control and reduces the overall computational burden. This work helps to enhance the participation of machine learning control algorithm in the field of renewable energy where so many parametric uncertainties are present.

Author Contributions

B.K. conceptualized the idea and the formulation to achieve the goal. B.K. developed the theory and simulated the model. R.S. validated and investigated the theory as well as data/results presented. K.S.S. supervised the work and review as well as edited the original draft. All the authors discussed the outcome and contributed to the manuscript.

References

- [1] IBRAHIM, N. Z., A. AL-QUTEIMAT, M. MOZUMDAR and S. AL JUFOUT. A novel approach for crowbar resistance determination for doubly fed induction generators in wind energy conversion systems. *International Journal of Ambient Energy*. 2021, pp. 1–10. ISSN 2162-8246. DOI: 10.1080/01430750.2021.1874519.
- [2] NIAN, H. and L. LI. Direct Power Control of Doubly Fed Induction Generator Without Phase-Locked Loop Under Harmonically Distorted Voltage Conditions. *IEEE Transactions on Power Electronics*. 2018, vol. 33, iss. 7, pp. 5836–5846. ISSN 1941-0107. DOI: 10.1109/TPEL.2017.2740265.
- [3] NAIR, R. and G. NARAYANAN. Stator Flux Based Model Reference Adaptive Observers for Sensorless Vector Control and Direct Voltage Control of Doubly-Fed Induction Generator. *IEEE Transactions on Industry Applications*. 2020,

- vol. 56, iss. 4, pp. 3776–3789. ISSN 1939-9367. DOI: 10.1109/TIA.2020.2988426.
- [4] XIONG, L., P. LI and J. WANG. High-order sliding mode control of DFIG under unbalanced grid voltage conditions. *International Journal of Electrical Power & Energy Systems*. 2020, vol. 117, iss. 1, pp. 1–13. ISSN 0142-0615. DOI: 10.1016/j.ijepes.2019.105608.
- [5] LI, S., T. A. HASKEW, Y.-K. HONG and L. XU. Direct-current vector control of three-phase grid-connected rectifier–inverter. *Electric Power Systems Research*. 2011, vol. 81, iss. 2, pp. 357–366. ISSN 0378-7796. DOI: 10.1016/j.epsr.2010.09.011.
- [6] AGHA KASHKOOLI, M. R., S. M. MADANI and T. A. LIPO. Improved Direct Torque Control for a DFIG under Symmetrical Voltage Dip With Transient Flux Damping. *IEEE Transactions on Industrial Electronics*. 2020, vol. 67, iss. 1, pp. 28–37. ISSN 1557-9948. DOI: 10.1109/TIE.2019.2893856.
- [7] ZHANG, Y., J. LIU, H. YANG and J. GAO. Direct Power Control of Pulsewidth Modulated Rectifiers Without DC Voltage Oscillations Under Unbalanced Grid Conditions. *IEEE Transactions on Industrial Electronics*. 2018, vol. 65, iss. 10, pp. 7900–7910. ISSN 1557-9948. DOI: 10.1109/TIE.2018.2807421.
- [8] SUN, D., X. WANG, H. NIAN and Z. Q. ZHU. A Sliding-Mode Direct Power Control Strategy for DFIG Under Both Balanced and Unbalanced Grid Conditions Using Extended Active Power. *IEEE Transactions on Power Electronics*. 2018, vol. 33, iss. 2, pp. 1313–1322. ISSN 1941-0107. DOI: 10.1109/TPEL.2017.2686980.
- [9] ZAREI, M. E., C. VEGANZONES NICOLAS and J. R. ARRIBAS. Improved Predictive Direct Power Control of Doubly Fed Induction Generator During Unbalanced Grid Voltage Based on Four Vectors. *IEEE Journal of Emerging and Selected Topics in Power Electronics*. 2017, vol. 5, iss. 2, pp. 695–707. ISSN 2168-6785. DOI: 10.1109/JESTPE.2016.2611004.
- [10] RUIZ-CRUZ, R., E. N. SANCHEZ, A. G. LOUKIANOV and J. A. RUZ-HERNANDEZ. Real-Time Neural Inverse Optimal Control for a Wind Generator. *IEEE Transactions on Sustainable Energy*. 2019, vol. 10, iss. 3, pp. 1172–1183. ISSN 1949-3037. DOI: 10.1109/TSTE.2018.2862628.
- [11] WANG, B., C. LIU, S. CHEN, S. DONG and J. HU. Data-Driven Digital Direct Position Servo Control by Neural Network With Implicit Optimal Control Law Learned From Discrete Optimal Position Tracking Data. *IEEE Access*. 2019, vol. 7, iss. 1, pp. 126962–126972. ISSN 2169-3536. DOI: 10.1109/ACCESS.2019.2937993.
- [12] DJILALI, L., E. N. SANCHEZ, F. ORNELAS-TELLEZ, A. AVALOS and M. BELKHEIRI. Improving Microgrid Low-Voltage Ride-Through Capacity Using Neural Control. *IEEE Systems Journal*. 2020, vol. 14, iss. 2, pp. 2825–2836. ISSN 2373-7816. DOI: 10.1109/JSYST.2019.2947840.
- [13] KHARCHOUF, I., T. NASSER, A. ESSADKI and M. FDAILLI. Adaptive Fuzzy-PI Control of Wind Energy Conversion System Based DFIG Under Voltage Dip. In: *2020 International Conference on Electrical and Information Technologies (ICEIT)*. Rabat: IEEE, 2020, pp. 1–6. ISBN 978-1-72814-341-5. DOI: 10.1109/ICEIT48248.2020.9113215.
- [14] LAI, Y.-S. and J.-C. LIN. New hybrid fuzzy controller for direct torque control induction motor drives. *IEEE Transactions on Power Electronics*. 2003, vol. 18, iss. 5, pp. 1211–1219. ISSN 1941-0107. DOI: 10.1109/TPEL.2003.816193.
- [15] JALADI, K. K. and K. S. SANDHU. Real-Time Simulator based hybrid control of DFIG-WES. *ISA Transactions*. 2019, vol. 93, iss. 1, pp. 325–340. ISSN 0019-0578. DOI: 10.1016/j.isatra.2019.03.024.
- [16] SAIDI, A. S. and W. HELMY. Artificial neural network–aided technique for low voltage ride-through wind turbines for controlling the dynamic behavior under different load conditions. *Wind Engineering*. 2019, vol. 43, iss. 4, pp. 420–440. ISSN 2048-402X. DOI: 10.1177/0309524X18791387.
- [17] LIN, F.-J., K.-C. LU, T.-H. KE, B.-H. YANG and Y.-R. CHANG. Reactive Power Control of Three-Phase Grid-Connected PV System During Grid Faults Using Takagi–Sugeno–Kang Probabilistic Fuzzy Neural Network Control. *IEEE Transactions on Industrial Electronics*. 2015, vol. 62, iss. 9, pp. 5516–5528. ISSN 1557-9948. DOI: 10.1109/TIE.2015.2407851.
- [18] ADOUNI, A., D. CHARIAG, D. DI-ALLO, M. B. HAMED and L. SBITA. FDI based on Artificial Neural Network for Low-Voltage-Ride-Through in DFIG-based Wind Turbine. *ISA Transactions*. 2016, vol. 64, iss. 1, pp. 353–364. ISSN 0019-0578. DOI: 10.1016/j.isatra.2016.05.009.

- [19] DE MARCHI, R. A., P. S. DAINEZ, F. J. VON ZUBEN and E. BIM. A Multi-layer Perceptron Controller Applied to the Direct Power Control of a Doubly Fed Induction Generator. *IEEE Transactions on Sustainable Energy*. 2014, vol. 5, iss. 2, pp. 498–506. ISSN 1949-3037. DOI: 10.1109/TSTE.2013.2293621.
- [20] ZOU, J., C. PENG, H. XU and Y. YAN. A Fuzzy Clustering Algorithm-Based Dynamic Equivalent Modeling Method for Wind Farm With DFIG. *IEEE Transactions on Energy Conversion*. 2015, vol. 30, iss. 4, pp. 1329–1337. ISSN 1558-0059. DOI: 10.1109/TEC.2015.2431258.
- [21] MOHAMMADI, J., S. VAEZ-ZADEH, S. AF-SHARNIA and E. DARYABEIGI. A Combined Vector and Direct Power Control for DFIG-Based Wind Turbines. *IEEE Transactions on Sustainable Energy*. 2014, vol. 5, iss. 3, pp. 767–775. ISSN 1949-3037. DOI: 10.1109/TSTE.2014.2301675.

About Authors

Brijesh KUMAR was born in Jaunpur, India. He received his M.Tech. from Kurukshetra National Institute of Technology (KNIT) Sultanpur in 2011. His research interests include electrical machine and drives, Renewable Energy.

Kanwarjit Singh SANDHU was born in Jaunpur, India. He received his M.Tech. from KNIT Sultanpur in 2011. His research interests include electrical machine and drives, Renewable Energy.

Rahul SHARMA was born in Bareilly, India. He is received his B.Tech degree from KNIT Sultanpur, M.Tech from MNNIT Allahabad and Ph.D. from NIT Kurukshetra. He is current assistant professor in NIT Kurukshetra, India. His area of interest includes renewable energy systems, power electronics control and electrical drives.